Real-time monitoring of casein gel microstructure during simulated gastric digestion monitored by small-angle neutron scattering

Meltem Bayrak, Andrew E Whitten, Jitendra P Mata, Charlotte E Conn, Juliane Floury, Amy Logan

Food Hydrocolloids 144 (2023) 108919

Contents lists available at ScienceDirect

Food Hydrocolloids

journal homepage: www.elsevier.com/locate/foodhyd

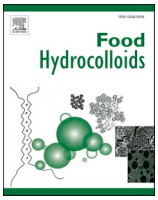

Real-time monitoring of casein gel microstructure during simulated gastric digestion monitored by small-angle neutron scattering

Meltem Bayrak [a,c], Andrew E. Whitten [b], Jitendra P. Mata [b], Charlotte E. Conn [c], Juliane Floury [d], Amy Logan [a,*]

[a] CSIRO Agriculture and Food, 671 Sneydes Road, Werribee, Victoria, 3030, Australia
[b] Australian Centre for Neutron Scattering (ACNS), Australian Nuclear Science and Technology Organisation (ANSTO), Lucas Heights, NSW, 2234, Australia
[c] School of Science, College of Science, Engineering and Health, RMIT University, 124 LaTrobe Street, Melbourne, VIC, 3000, Australia
[d] STLO, INRAE, Institut Agro, 35042, Rennes, France

ARTICLE INFO

Keywords:
In *situ* digestion
Rennet
Transglutaminase
Gel
Flow setup
Small and ultra-small angle neutron scattering (SANS and USANS)

ABSTRACT

The evolving structure of protein-based foods during the digestion process is critical to the release of nutrients. However, traditional *in vitro* monitoring of the gel micro- and nano-structure during digestion involves analysing sample aliquots taken at different digestion time periods. This can pose issues for some gels, such as casein-based gels, as they are sensitive to sample manipulation and environmental changes. Herein, a newly developed flow setup was utilised to monitor (at the micro- and nano-length scales) the gel protein network of rennet-induced (RG) and transglutaminase-induced acid gels (TG) *in situ* and in real-time during simulated gastric digestion using ultra-small and small-angle neutron scattering (USANS and SANS). The proteolysis kinetics of the gels were investigated at two different pepsin enzyme concentrations (2000 and 8000 U mL^{-1}) and in two different solvent environments (H_2O and D_2O). Results indicate that the flowing *in situ* system had a greater effect on the microstructural breakdown of TG relative to the acid-sensitive RG, compared to the traditional static method. This is the first *in situ* digestion study observing the structural changes of large protein gel particles with USANS or SANS in real-time. Our findings advance the understanding of the kinetics of casein gel disintegration under simulated conditions of gastric digestion relating to pepsin enzyme concentration and solvent environment, and critically, the utilisation of a new *in situ* and real-time setup for neutron studies.

1. Introduction

The structure of protein-based foods plays a critical role in determining their fate during gastric digestion as nutrients entrapped in the food matrix are released as a result of mechanical and enzymatic breakdown and the effect of an acidic environment (Boland, Golding, & Singh, 2014; Hong & Salentinig, 2022; Norton, Wallis, Spyropoulos, Lillford, & Norton, 2014; Singh, Ye, & Ferrua, 2015). Therefore, the structure of the protein gel in the digestive environment defines its breakdown under gastric conditions, relating to its digestion rate. Although only a small amount of protein is digested in the stomach, gastric emptying controls the rate of digestion and is particularly important for the postprandial response (Bornhorst, Ferrua, & Singh, 2015; Kong & Singh, 2009; Mackie, Rafiee, Malcolm, Salt, & van Aken, 2013; Somaratne et al., 2020; Ye, Cui, Dalgleish, & Singh, 2016). For example, slow rates of peptide and amino acid release during protein digestion are more effective at prolonging satiety, improving insulin response, and decreasing postprandial serum glucose levels (Claessens, Calame, Siemensma, van Baak, & Saris, 2009; Morifuji et al., 2010) which benefit people suffering from obesity and diabetes. On the other hand, rapid digestion of protein sources, such as protein hydrolysates compared to intact protein, can be particularly helpful for ageing people with declining muscle mass for rapid muscle protein synthesis (Calbet & Holst, 2004; Dangin; Boirie; Guillet, & Beaufrère, 2002; Dangin et al., 2003; Morifuji et al., 2010).

Protein digestion begins in the stomach with mechanical, chemical, and enzymatic breakdown steps; namely, mechanical sheer of mixing by the stomach and proteolysis by pepsin in the acidic gastric environment (Bornhorst, Gouseti, Wickham, & Bakalis, 2016). Protein structures are sensitive to the enzymatic and acidic effects of the stomach environment, as well as to the mechanical effects of the digestive system, with varying degrees of sensitivity to each element depending on the

* Corresponding author. CSIRO Agriculture and Food, 671 Sneydes Road, Werribee, Victoria, 3030, Australia.
E-mail address: amy.logan@csiro.au (A. Logan).

https://doi.org/10.1016/j.foodhyd.2023.108919
Received 2 December 2022; Received in revised form 17 May 2023; Accepted 25 May 2023
Available online 5 June 2023

structure. Mechanical breakdown, during which particle size decreases and surface area increases, results in an increase in hydrolysis mostly owing to the diffusion of pepsin on a larger surface area and is a critical digestion step (Bayrak et al., 2021; Grassby et al., 2017; Grundy et al., 2015; Lyu et al., 2021; Mandalari et al., 2018). Studying the impact of mechanical breakdown and incorporating it into digestion studies is also essential, as particle size, structure and brittleness can impact how gel structure responds to mechanical disruption (Farooq et al., 2018; Jalabert-Malbos, Mishellany-Dutour, Woda, & Peyron, 2007; Y. Li, Li, Wang, & Li, 2022; Liu, Dhital, Wu, Chen, & Gidley, 2019).

Casein represents about 80% of the protein content in bovine milk and is the primary structural component of most dairy products consumed. The casein micelle, which consists of four casein proteins (α_{s1}-casein, α_{s2}-casein, β-casein, κ-casein) is a good model for studying structure-function relationships due to its ability to form gels with a variety of different structures under environmental instability. Different mechanisms of gelation, such as changing the κ-casein surface layer interactions or the loss of colloidal calcium phosphate, result in the formation of a wide variety of casein gel structures with the same composition. The structure of these gels can be further modified by the introduction of covalent cross-linking, using enzymes such as transglutaminase. Some studies have used small-angle X-ray scattering (SAXS) or small-angle neutron scattering (SANS), combined with rheology, electron microscopy, deep-UV fluorescence microscopy and other techniques to study the structure of casein and casein gels (Bayrak et al., 2021; Bouchoux, Gesan-Guiziou, Pérez, & Cabane, 2010; Callaghan-Patrachar, Peyronel, Pink, Marangoni, & Adams, 2021; Floury et al., 2018; Holt, De Kruif, Tuinier, & Timmins, 2003; Ingham et al., 2016; Lazzaro et al., 2020; Q. Li & Zhao, 2019; Mata, Udabage, & Gilbert, 2011; Roefs, de Groot-Mostert, & Van Vliet, 1990). The behaviour of rennet-induced gels (RG) and transglutaminase-induced acid gels (TG) on the micro and nanoscale has been previously characterised under static conditions; where the homogeneous but more brittle TG structure was found to be more resistant to digestion compared to the elastic RG structure (Bayrak et al., 2021). RG is associated with strong aggregation and the formation of tight coagulum due to acid syneresis in the gastric environment, resulting in lower pepsin accessibility and a slower release of nutrients (Barbé et al., 2014; Floury et al., 2018). While the behaviour of casein gels during gastric digestion is known to be affected by their sensitivity to an acidic environment, brittleness and resistance to shear, these effects have not yet been characterised with time *in situ* at the nanoscale level.

To date, flowing *in situ* digestion measurements using scattering techniques have been limited to liquid-like systems (Hong and Salentinig, 2022), such as milk (Clulow, Salim, Hawley, & Boyd, 2018; Salentinig, Phan, Hawley, & Boyd, 2015; Salentinig, Phan, Khan, Hawley, & Boyd, 2013), lipids (Fatouros et al., 2007; Khan, Hawley, Rades, & Boyd, 2016; Rezhdo et al., 2017; Warren, Anby, Hawley, & Boyd, 2011; Yaghmur et al., 2019), mayonnaise (Salentinig, Amenitsch, & Yaghmur, 2017), cellulose dispersions (Kent et al., 2010), and starch granules dispersed in buffer (Blazek & Gilbert, 2010). Due to the experimental constraints of neutron scattering, the time-dependent behaviour of solid-like food structures is experimentally more difficult; it is, therefore, typically measured by stopping the enzymatic reaction during static experiments, placing the solid sample in a sample holder, and running the measurement. A previous study by Bayrak et al. (2021) used this technique by removing casein gel digesta samples at various time points during digestion following the static INFOGEST protocol (Brodkorb et al., 2019) to be examined with USANS and SANS. However, to our knowledge, small-angle scattering has not yet been used to determine the *in situ* structural changes of a gel during digestion at the micro- and nanoscale.

To overcome this limitation, a newly developed flow cell was utilised to conduct temperature and pH-controlled digestion while allowing gel particles to flow through the cell using a pump (Bayrak et al., 2022).

This study aimed to achieve a real-time *in vitro* gastric digestion setup focusing on casein gels' enzymatic and mechanical devolution/disruption at the micro- and nanoscales using USANS and SANS, to contribute to a better understanding of the digestion kinetics of protein-based foods. A novel continuous *in situ* flow setup for gastric *in vitro* digestion experiments was developed based on the static (Brodkorb et al., 2019) and semi-dynamic INFOGEST approach developed by Mulet-Cabero et al. (2020), allowing structural changes to be monitored in real-time over 240 min of digestion. The setup was developed for neutron scattering rather than X-rays (e.g., SAXS) as the focus of this investigation was the devolution of the casein gel network structure. In contrast, a SAXS study would be dominated by the calcium signal of the calcium phosphate nanoclusters, therefore providing information predominantly on the internal structure of the casein micelles. In addition, neutrons are non-invasive and can be used without affecting the sample's structure, which is particularly important for studies collected over longer periods of time, where preliminary studies have shown continual exposure to X-rays can lead to sample degradation (data not shown). Moreover, the neutron scattering instrumentation at ANSTO utilised for the current work provides access to both SANS and USANS in combination to obtain complimentary structural information from length scales of 1 nm–20 μm which is not possible using SAXS-USAXS.

Herein, we focused on TG and RG casein gels whose digestion kinetics with pepsin have been characterised (from macro-to nanoscales) and reported previously using the static INFOGEST model (Bayrak et al., 2021). Moreover, TG and RG are of importance to the dairy industry, representing the formation and structural properties of yoghurt and cheese, respectively. With the knowledge that blending will decrease particle size and increase surface area, thereby potentially altering the kinetics, digestion was examined using various pepsin enzyme concentrations (2000 and 8000 U mL^{-1}) in H_2O and D_2O, solvents that are known to contribute to the formation of the gel network matrix. The objective of this work was to; (1) validate a new *in situ* model for future neutron studies with solid or semi-solid particles, (2) study the kinetics and structural changes of RG and TG in the presence of different concentrations of pepsin enzyme and different solvent environments (H_2O and D_2O) under simulated gastric digestion conditions in real-time.

2. Materials and methods

2.1. Materials

Micellar casein powder (MCP, Prodiet 85B), from Ingredia (Arras, France), with 82.4% w/w protein, was used in this study. Transglutaminase (ACTIVA WM; 100 U g^{-1}) was kindly supplied by Ajinomoto Co., Inc. (Tokyo, Japan). Chymosin, the primary enzyme in rennet (CHY-MAX® Plus; 200 IMCU mL^{-1}) was purchased from Chr. Hansen Pty. Ltd. (Bayswater, Victoria, Australia). Pepsin from porcine gastric mucosa (P6887), deuterium oxide (D_2O; 151882), pepstatin A (P5318), D-(+)-Gluconic acid δ-lactone (G4750), the haemoglobin from bovine blood (H6525) and all other chemicals were purchased from Sigma-Aldrich, Inc (St. Louis, MO, USA). The pepsin activity in H_2O and D_2O was determined using the standardised pepsin activity assay (EC 3.4.23.1) with haemoglobin as a substrate as reported previously by Bayrak et al. (2021); Brodkorb et al. (2019).

2.2. Methods

2.2.1. Preparation of casein gels from micellar casein powder

The MCP was solubilised, and the gels were prepared according to the method of Bayrak et al. (2021). In brief, MCP 10% (w/w) solution was rehydrated in H_2O or D_2O, achieving >98% solubilisation. Sodium azide (0.02% (w/w)) was added to the solution to prevent microbial growth. For the transglutaminase-induced acid gel (TG), the pD of the MCP solution in D_2O was adjusted with DCl/NaOD to match the pH of the solution in H_2O, and then transglutaminase powder (5 U g^{-1} final concentration) and 1.1% (w/w) glucono-∂-lactone (GDL) was added to

the MCP solution. The rennet-induced acid gel was formed by adjusting the pH or pD of the MCP solution to 6.5 and adding Chymosin (0.03 International Milk Clotting Unit (IMCU) mL^{-1} final concentration).

2.2.2. Preparation of casein gel blends in simulated digestive fluid

The simulated salivary fluid (SSF, pH/pD 7) and simulated gastric fluid (SGF, pH/pD 3) were prepared according to Brodkorb et al. (2019). Following the INFOGEST static digestion protocol, the oral phase would normally involve the dilution of food materials 1:1 (w/w) with SSF for 2 min with mixing, followed by a further 1:1 (v/v) dilution with SGF prior to the addition of pepsin. For this experiment, the oral and gastric phases were combined into one due to the inability to access the equipment during the *in situ* measurements behind the radiation shielding and sequentially add each phase. To obtain a continuous flow in the flow cell system, the gels were blended into the digestive fluid. For the flow setup, a block of gel sample (40 g) was combined with SSF (20 mL), SGF (32 mL) and HCl/DCl (4 mL, to maintain a pH of 3) in a beaker. The amount of gel sample used in the current study was double the ratio specified in the INFOGEST protocol, and used previously by Bayrak et al. (2021), to maximise the signal-to-noise ratio of the neutron scattering data for short collection times. For gels in D_2O, SSF and SGF were prepared in 100% D_2O, similar to Bayrak et al. (2021). A slight variation was used for gels in H_2O where SSF and SGF were prepared in 'air-contrast matched water' (ACMW, 8% D_2O) resulting in a scattering length density of zero, thereby avoiding scattering from any air bubbles generated during the water flow. This common approach in neutron scattering has proven to have a negligible effect on structure when significant excess of H_2O is used in mixtures of normal and heavy water (Stefaniuk et al., 2022). It was necessary to reduce the gel particle size to ensure the particles flowed continuously through the sample cell of the *in situ* flow system. For this purpose, a recent study established that the scale of deformation caused by blending a TG gel in simulated digestive fluid for up to 10 s did not affect the micro and nanostructure of the gel network probed by USANS and SANS (Bayrak et al., 2022). As such, the particle size obtained herein by blending (~1 mm on average) ensured that the gel-digestive fluid mixture was suitable for the *in situ* study without leading to a structural change in the interior of the gel particle (Bayrak et al., 2022). Mechanical disruption during the oral phase was not included here, as necessary particle reduction was caused by blending. Although, SSF was not eliminated and combined with SGF to maintain a constant salt concentration in the solution.

2.2.3. An in situ flow setup for the real-time USANS and SANS analysis of simulated gastric digestion

The USANS and SANS measurements were performed on the Kookaburra and Bilby beamlines respectively at the OPAL reactor (Rehm et al., 2018; Sokolova et al., 2019), as described previously by Bayrak et al. (2022). The USANS measurements were performed to cover a q-range of 3.5×10^{-5} Å^{-1} to 0.008 Å^{-1}, using a long wavelength of 4.74 Å (high flux mode). The SANS collection was performed in time-of-flight mode with a wavelength range of $\lambda = 2$–20 Å, and a wavelength resolution of $\Delta\lambda/\lambda = 0.12$. With an array of detectors positioned at 7.000 m, 3.000 m and 2.000 m, a q-range of 0.002–0.55481 Å^{-1} was covered in a single measurement. The collimation length used was 6.800 m and the source and sample apertures were both circular with diameters of 40 mm and 12.5 mm, respectively. USANS raw data were reduced and normalised to an absolute scale (slit smeared data) using an in-house developed Python script in Gumtree software. SANS data reduction was carried out using Mantid, data analysis and a visualisation package (Arnold et al., 2014).

The newly developed experimental configuration for the *in situ* analysis of soft material particles via neutron scattering is shown in Fig. 1 (Bayrak et al., 2022). The blended gel particles in the simulated digestive fluid were poured into the reaction vessel and circulated through the sample cell (1 mm in path length) and back into the reaction vessel via silicone tubing (2 mm in diameter) using a Gilson Minipuls peristaltic pump (10 mL min^{-1} flow rate, to replicate conditions of Egger et al. (2019), creating a laminar flow according to the Reynolds number calculated. The sample environment requires a sample cell path length of 1 mm to avoid any multiple scattering yet wide enough for the flow of semi-solid gel particles, from which real-time data can be collected to probe changes in the micro and nanostructure during digestion. The tubing is connected to the bottom of the reaction vessel to ensure that settled gel particles are pumped around the flow setup along with the other material (Fig. 2). A copper coil water heater was wrapped around the reaction vessel to maintain a reaction temperature of 37 °C. No

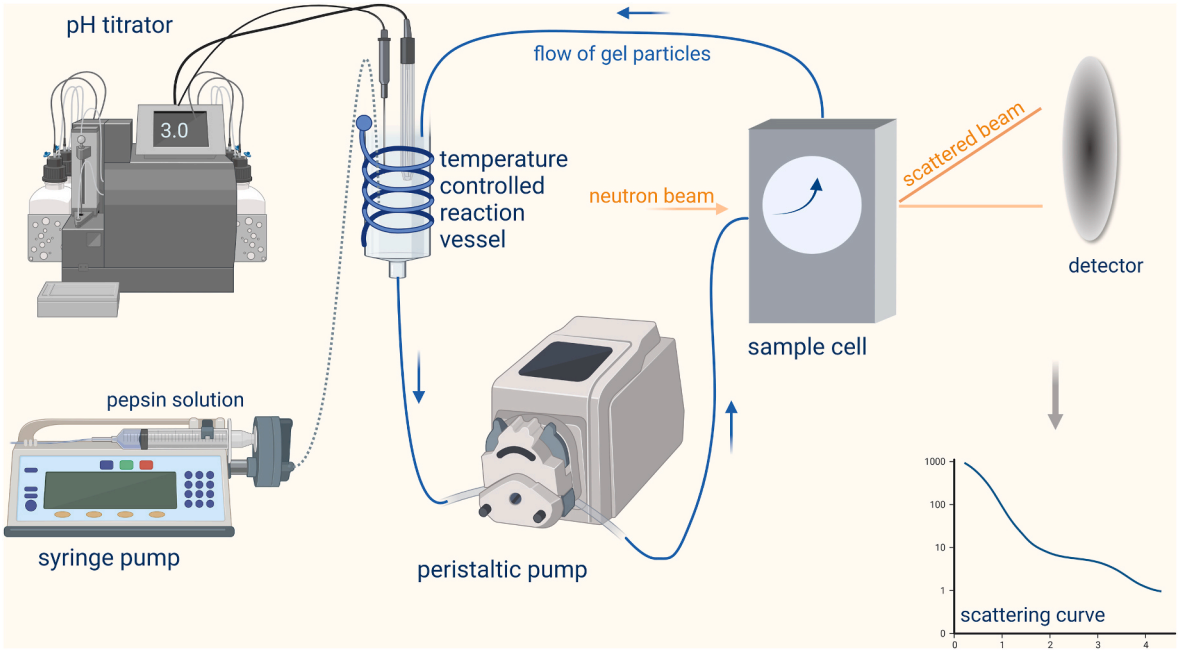

Fig. 1. Schematic representation of the 1 experimental flow setup used for the *in situ* study of the digestion of casein gels using ultra-small (USANS) and small-angle neutron scattering (SANS).

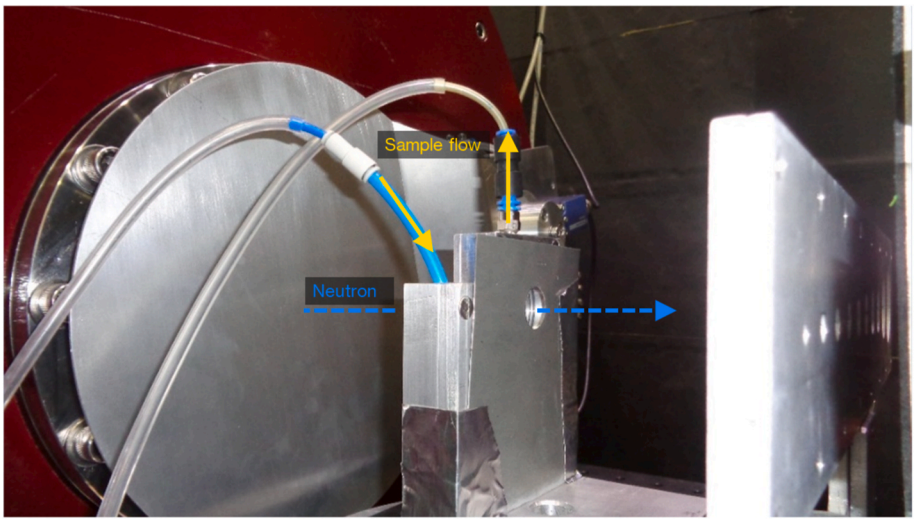

Fig. 2. Sample cell positioned on the SANS beamline. The sample flow is indicated using the yellow arrows; into the sample cell from the side (blue tubing) and exiting through the top, returning into the temperature-controlled reaction vessel. Photo Credit: Australian Nuclear Science and Technology Organisation (ANSTO, Lucas Heights, NSW Australia).

stirring was required as the agitation caused by the flow of the solution through the tubing was sufficient for mixing. The pH or pD of the solution in the reaction vessel was maintained at 3 throughout the experiment using a pH titrator (1M HCl and 1M NaOH). The flowing gel particles in the gastric fluid were allowed to circulate for 1 h, during which SANS data were collected, representing a control measurement. After 1 h, pepsin enzyme (2000 U mL^{-1} or 8000 U mL^{-1} [in H_2O and D_2O]) was added to the gastric fluid remotely using a syringe pump to allow for data to be collected from time zero (T0) of simulated digestion. The flowing gel particles, gastric fluid and pepsin were allowed to circulate for a further 240 min to simulate gastric digestion. Neutron scattering data were averaged over 10 min intervals. The digestion reaction was halted by the addition of a pepsin enzyme inhibitor, Pepstatin A (1 mL, 0.5 mg mL^{-1}), after which the structure of the flowing gel particles in the inactivated system were investigated for an additional 1 h.

RG and TG samples exposed to simulated gastric digestion with adjusted enzyme activity (2000 U mL^{-1} or 8000 U mL^{-1}) in H_2O or D_2O were analysed. Modelling of the SANS data was performed using SasView software using the correlation length model (http://sasview.org) (Hammouda, Ho, & Kline, 2004). For low q SANS data, the intensity decrease at a single q value was fitted to a regression equation $I(q, t) = I(q, t = 0)\exp(-Rt)$, where I is the intensity and R is the rate constant of network disruption. A regression equation $I(q = 0.002, t) = I(q = 0.002, t = 0)\exp(-Rt)$, was fitted to the scattered intensity vs time using R studio, where $I(q = 0.002, t)$ is the intensity at $q = 0.002$ at time t, $I(q = 0.002, t = 0)$ is the intensity at time 0, and R is the rate constant of gel network disruption.

2.2.4. Statistical analysis

Results were analysed statistically using RStudio v3 software (RStudio™, Boston, MA, USA) with the "TukeyHSD" function. One-way analysis of variance (ANOVA) was performed to measure differences. $P \leq 0.01$ was considered statistically significant.

3. Results

3.1. Study on digestion kinetics of casein gels

To understand the kinetics of casein gel breakdown up to the micrometre scale, intensity changes in the low q region of the SANS instrument Bilby were investigated with time at four different q values (0.002 $Å^{-1}$, 0.003 $Å^{-1}$, 0.004 $Å^{-1}$,0.005 $Å^{-1}$) for pepsin concentrations of 2000 U mL^{-1} and 8000 U mL^{-1} at pH/pD 3. A similar kinetic trend was observed for low q values (Figs. S1 and S2 for q 0.002 and 0.003 $Å^{-1}$) indicating that changes occur to the gel structure with time at the aggregated micelle length scale (0.0020 $Å^{-1}$ = 314 nm to 0.0050 $Å^{-1}$ = 126 nm). 0.0020 $Å^{-1}$ was the smallest q value measured with Bilby in the current work and was selected to investigate the structural variation occurring close to a micrometre scale.

The values for R (relating to the rate at which the scattering intensity decreases over time) and A (the scale factor, defined as the extrapolated intensity at $t = 0$) measured using regression analysis for samples at $q = 0.002$ are presented in Table 1. Changes in the rate of protein hydrolysis, hence digestion, are reflected in changes in the rate at which scattering decreases over time, given by the R coefficient in the regression equation. Here, a higher R value indicates a greater rate of digestion over time. The R values increased with increasing pepsin concentration for all samples, except for RG-H, where the digestion rate was higher at 2000 than at 8000 U mL^{-1}. Overall, the highest R value was measured for RG-H digested in the presence of 2000 U mL^{-1} pepsin, followed by TG-D with 8000 U mL^{-1}, which is related to gel structure and is explored further in the discussion section. No change in the $I(q = 0.002)$ value was observed for TG-H with time in the presence of 2000 U mL^{-1} pepsin demonstrated by an R value of about 0, indicating limited digestion. However, a small increase in R value with time was observed for TG-H with 8000 U mL^{-1} pepsin, suggesting a slight increase in digestion rate at the higher pepsin concentration. The scale factor (A) is linked to the contrast of the gel (the contrast of the gel in D_2O is higher than for H_2O), and the amount of gel that flows through the cell during a given time interval. This makes meaningful interpretation and comparison of A from different samples difficult. Instead, intensity versus time measurements are shown to be an effective tool for assessing the aggregation kinetics of gel or protein network systems. For example, previous

Table 1
The R values of regression equation $y = A.\exp(-Rt)$ as $I(q = 0.002, t) = I(q = 0.002, t = 0)\exp(-Rt)$, fitted to $I(q)$ vs time of SANS data collected during *in vitro* gastric digestion with 2000 U mL^{-1} and 8000 U mL^{-1} pepsin.

Sample	2000 U mL^{-1}	8000 U mL^{-1}
RG-H	0.052 ± 0.004	0.014 ± 0.001
RG-D	0.0033 ± 0.0001	0.0052 ± 0.0002
TG-H	−0.0008 ± 0.0002	0.0024 ± 0.0002
TG-D	0.0111 ± 0.0006	0.030 ± 0.003

scattering investigations have measured changes in scattering intensity as a function of time for a given q range to quantify the gelation process (Huang, Terech, Raghavan, & Weiss, 2005), structural change in steels (Nishijima, Tomota, Su, Gong, & Suzuki, 2016) or electrochemical gelation (Randle et al., 2022) and the method has been shown to be an effective tool for assessing time-dependent kinetics. It should be noted that the Kookaburra instrument uses an analyser crystal that must change position to collect data for each q value, therefore the acquisition of data over a wider q-range at short intervals of time is not possible. However, monitoring absolute intensity change at one q value is achievable by fixing the analyser crystal angle. Kookaburra was used to analyse a representative TG-H gel and the full scattering spectra before digestion, after digestion, and the absolute intensity at one q value of 7.6×10^{-5} during digestion was measured. Fig. 3A depicts the spectra, while Fig. 3B illustrates the intensity change over time when digested with 8000 U mL^{-1} pepsin. The length scale at this q value is approximately 8 μm. When digested with 2000 U mL^{-1} pepsin, only a slight change in structure was observed; however, 8000 U mL^{-1} pepsin caused a significant breakdown.

3.2. Time-resolved structural changes during gastric digestion using SANS

To investigate changes to the structure of RG and TG with time on the nanometer scale, SANS patterns were obtained in the q range of 0.002–0.5 Å^{-1} every 10 min during the digestion process using the Bilby SANS instrument and are provided in Figs. 4 and 5 for RG and TG, respectively. Two different pepsin enzyme concentrations (2000 U mL^{-1} and 8000 U mL^{-1}) were utilised to observe the kinetic effect in both H_2O and D_2O. Changes in the scattering pattern observed at lower q values reflect protein aggregation within the gel structure, while higher q values reveal protein clusters within casein micelles. One must fit a model to quantitatively evaluate the structural changes that have occurred. In our previous work (Bayrak et al., 2021), three distinct models were optimised to fit the scattering pattern of casein gels across a broad length scale (derived from combining USANS and SANS data). As the purpose herein is to demonstrate the feasibility of the newly developed *in situ* model and track the kinetics of changes in structure with time, a more simplistic model with fewer parameters was fitted to the scattering patterns across the entire SANS q range studied. As a result, a correlation length model, developed by Hammouda et al. (2004) for polymer solutions and hydrogel systems, was used to investigate structural differences with time (Fig. S3). The correlation length model has recently been used to explain several polymer and gel studies (Frieberg et al., 2018; Xu et al., 2021; Yang, Tyler, Ahrné, & Kirkensgaard, 2021, 2022; Yang et al., 2016). The model has also been used for inter-nanocluster interference (Mata et al., 2011). The equation for the correlation length model is:

$$I(q) = \frac{A}{q^n} + \frac{C}{1 + (q\xi)^m} + background \quad \text{(Equation 1)}$$

The Porod scattering term (A/q^n) describes the clustering strength from larger clusters like protein aggregates within the gel structure, where the Porod exponent (n) characterizes the fractal nature of a gel (Hammouda et al., 2004; Hammouda, Horkay, & Becker, 2005). Fig. 6 presents the clustering strength A/q^n for RG and TG digested in the presence of 2000 or 8000 U mL^{-1} pepsin as a function of time. The Porod exponent (n) was kept around 4, consistent with the smooth fractal surface of the gel, and the clustering strength is therefore determined mainly by the Porod scale (A). In this case, a low clustering strength may indicate the presence of dissolved chains, while a high clustering strength corresponds to the formation of networks and is therefore related to the degree of protein aggregation (Hammouda et al., 2004; Hammouda et al., 2005; Rasid, Do, Holten-Andersen, & Olsen, 2021; Saffer et al., 2014). The results indicate that, in general, the clustering strength decreases with digestion time. The only exception to this was TG-H digested with 2000 U mL^{-1} pepsin where the clustering strength increased slightly with time. In addition, all gels (again except for TG-H) reached a similar clustering strength after 240 min of digestion whether or not they were exposed to 2000 or 8000 U mL^{-1} pepsin. However, the concentration of pepsin appeared to affect the clustering strength during the early phases of gastric digestion, particularly RG-H and TG-D, exhibiting an immediate decrease in clustering strength that correlates with the greater effect observed in the digestion rates (R values) for SANS.

The change in correlation length for RG and TG digested in the presence of 2000 or 8000 U mL^{-1} pepsin as a function of time is shown in Fig. 7. The second term in equation (1) is a Lorentzian function, where the Lorentzian exponent (m) describes the polymer-solvent interactions, and the correlation length (ξ) characterizes the protein chain network. As such, the correlation length (ξ) usually provides an estimate of the average distance between the entanglement or connection points of the chain network, and the model has been used to measure pore size within the mesh structure. Here, a high degree of chain entanglement would lead to smaller channels or pores within the gel network and be reflected in a low ξ value. However, the correlation length values obtained in the current study were much smaller, in the range of 1.4 nm–5.3 nm, whereas casein gel pore sizes are generally on a micrometre scale (Bayrak et al., 2021; Schorsch, Jones, & Norton, 2002; Zhang et al.,

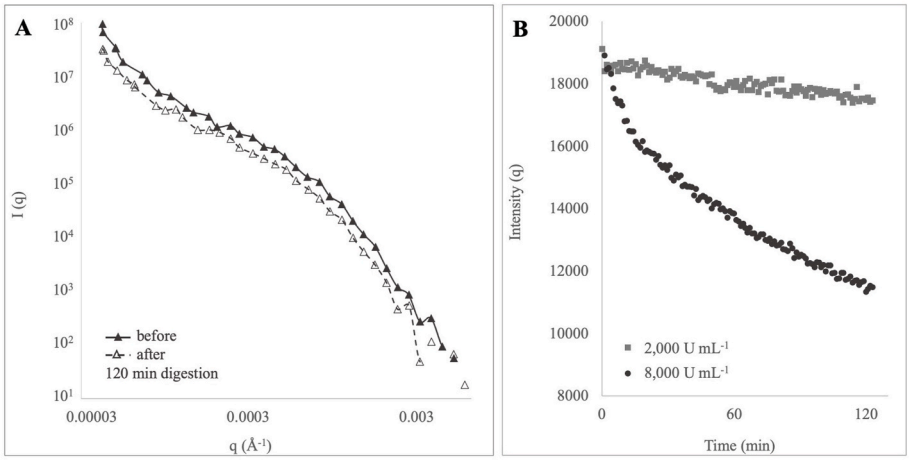

Fig. 3. (A) USANS scattering curves of TG-H with 8000 U mL^{-1} pepsin before (line) and after (dashed line) 120 min digestion. The USANS data were not desmeared prioritising the extraction of kinetic information over conducting a detailed structural analysis. (B) The intensity decrease at q of 7.6 x 10-5 Å over time of TG-H digested with 2000 mL^{-1} and 8000 U mL^{-1} pepsin (the y-axis has been shifted for both samples to have the same starting intensity).

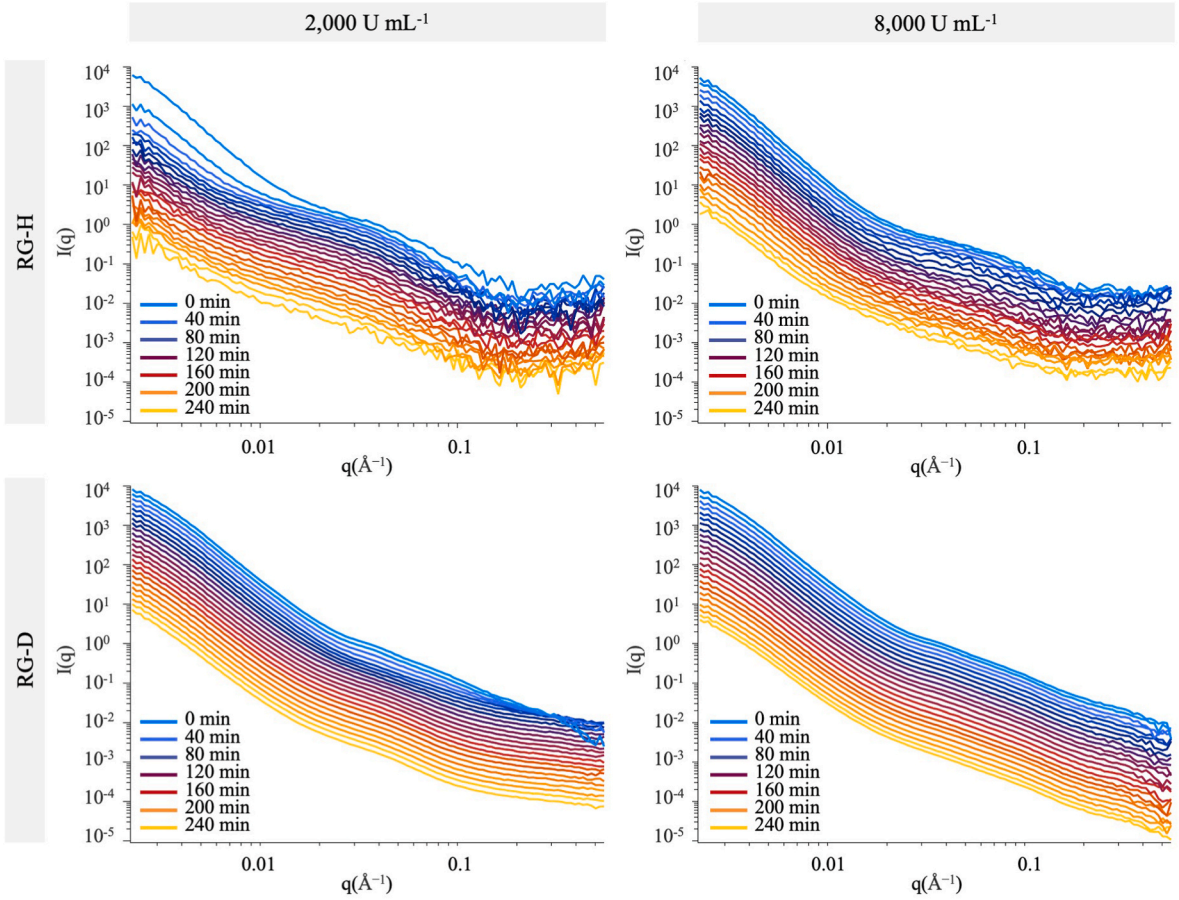

Fig. 4. *In situ* SANS profiles collected at time points during 240 min of *in vitro* gastric digestion of RG-H with 2000 U mL^{-1} pepsin (top left), RG-H with 8000 U mL^{-1} pepsin (top right), RG-D with 2000 U mL^{-1} pepsin (bottom left), and RG-D with 8000 U mL^{-1} pepsin (bottom right). SANS curves are vertically offset as a function of time by 100 absolute intensity units for clarity. As digestion progresses, the SANS profile colour changes from blue to red to yellow.

2017). For example, rennet-induced gels have been investigated with a pore size of 4–15 μm (Hussain, Bell, & Grandison, 2013; Mellema, Heesakkers, Van Opheusden, & Van Vliet, 2000) and the pore size of acid-induced casein gels has been found to be in the 1–10 μm range (Roefs et al., 1990). Here, correlation lengths at a nanometer length scale are believed to instead represent the average size, or local density, of the so-called inhomogeneous protein clusters (1–3 nm in size) arranged within the incompressible/hard regions (1–40 nm in size) of the casein micelle, as defined by Bouchoux et al. (2010) and Ingham et al. (2016), and more recently supported through the work of S. Yang, Tyler, Ahrné, and Kirkensgaard (2021). Saffer et al. (2014) measured correlation length values of a similar scale to that reported herein, between 2 and 13 nm, ascribed to the pore size of a gel, which presumably relates to changes in the organization of protein-stranded clusters within the interior of the casein micelle. While changes in scattering patterns for the 0.08–0.1 $Å^{-1}$ region have previously been associated with colloidal calcium phosphate nanoclusters (Bouchoux et al., 2010; Gebhardt, Takeda, Kulozik, & Doster, 2011; Marchin, Putaux, Pignon, & Léonil, 2007; Mata et al., 2011), De Kruif (2014) attribute these shifts in scattering to changes in the size of the protein inhomogeneities, as described herein, and reinforced by the work of Ingham et al. (2016) and Singh, Hemar, Gilbert, Wu, and Yang (2020). Initial correlation lengths for all samples were approximately 1.5–2.5 nm and increased in size up to around 5.5 nm after 240 min of digestion, indicating either an increase in the aggregation of small protein fragments or agglomeration of adjacent clusters within the hard regions of the micelle to form larger entities, with a corresponding increase in the size of water channels within a cluster (Bouchoux et al., 2010). The initial correlation length is slightly higher for gels in D_2O implying more aggregates or clusters of short peptides. In D_2O (Fig. 7a and b), the higher pepsin concentration of 8000 U mL^{-1} had only a small effect on the correlation length endpoint for RG, increasing slightly, whereas the correlation length for TG decreased with time. For 2000 U mL^{-1} pepsin in H_2O (Fig. 7c and d), TG showed no change in correlation length over time, but RG experienced an initial quick growth over the first 20 min followed by a slower rate of change compared to the steady increase observed for RG-H in the presence of 8000 U mL^{-1}, reaching the same level after 240 min regardless of pepsin concentration.

The inhomogeneous protein structure was also modelled by substructures with a simple spherical form (Sørensen, Pedersen, Mortensen, & Ipsen, 2013) using a modified Debye-Büche term (S. Yang, Tyler, et al., 2021). However, preliminary fitting showed no significant advantages in using this model over the correlation length model. It should be noted that the evolution of correlation length and clustering strength does not vary smoothly over time. The primary likely reason for this is that under the current setup, gel particles may become temporarily trapped in the cell or tubing, which may change the concentration and size distribution of gel particles passing through the neutron beam. Other smaller effects may stem from pH changes due to the buffering effect, or minor changes in the beam intensity (Figs. 6 and 7). Small variations at high q may be caused by changes in beam intensity and background subtraction, but they have no impact on the low q values (which are at least five orders of magnitude higher in intensity than the high q data) used to extract data for kinetic analysis. The variable effects should be addressed as the setup is optimised in future iterations.

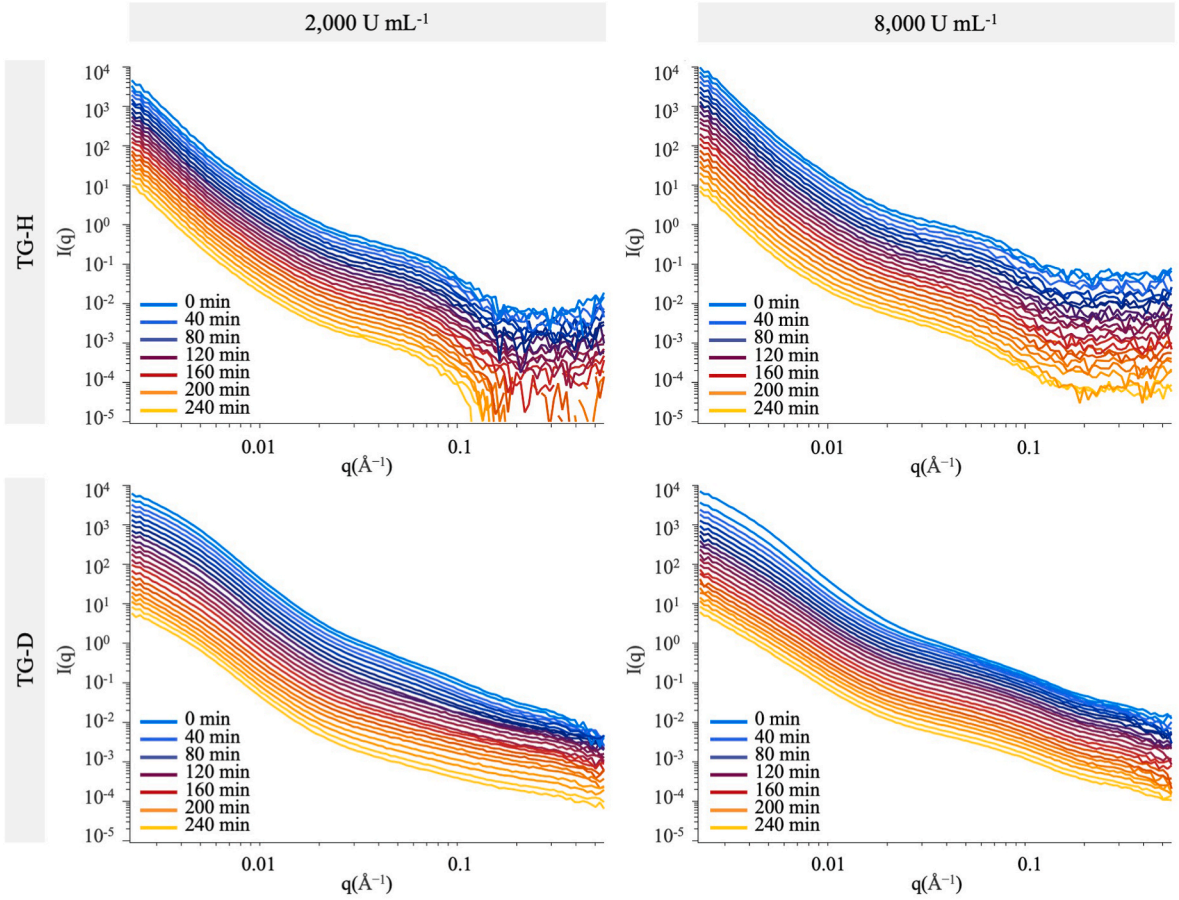

Fig. 5. *In situ* SANS profiles collected at time points during 240 min of *in vitro* gastric digestion of TG-H with 2000 U mL^{-1} pepsin (top left), TG-H with 8000 U mL^{-1} pepsin (top right), TG-D with 2000 U mL^{-1} pepsin (bottom left), and TG-D with 8000 U mL^{-1} pepsin (bottom right). SANS curves vertically offset as a function of time by 100 absolute intensity units for clarity As digestion progresses, the SANS profile colour changes from blue to red to yellow.

4. Discussion

This study set out to validate an *in situ* method to study the structural evolution of gels under flow and the instantaneous enzymatic action without sampling or the addition of inhibitors to stop enzymatic action using small-angle scattering. The *in situ* USANS and SANS data of blended casein gels submitted to pepsin digestion demonstrate that a detailed analysis of the structural evolution of semi-solid structures over time was possible using this setup. The structural changes observed during digestion as determined by SANS data are summarised as a schematic in Fig. 8. The results indicate that the degree of protein aggregation decreases with time for all gels during digestion, except for TG-H digested with 2000 U mL^{-1} pepsin demonstrated by an increase in clustering strength with time (Fig. 6). This suggests that the aggregated micelles in the protein gel network (on a hundreds of nanometer scale) are loosening due to the hydrolysis of the gel into smaller protein fragments, peptides, and amino acids. On the other hand, the correlation length (Fig. 7) tended to increase with time for all samples, again except for TG-H digested with 2000 U mL^{-1} pepsin and TG-D digested with 8000 U mL^{-1} which decreased slightly, suggesting that digestion increases the density of the protein-stranded clusters within the hard portions of the casein micelle for most samples. At a larger length scale, however, a loosening of gel aggregates was observed for TG-H. In Fig. 3A, the TG-H spectra do not appear significantly different before and after 120 min of digestion with 8000 U mL^{-1} pepsin, however, in Fig. 3B, the intensity is shown to decrease over time as digestion proceeds. In addition, low q SANS data demonstrated that the rate of aggregation kinetics of casein gels increased with increasing pepsin concentration for all samples, except for RG-H, which decreased from 0.052 to 0.14 U mL^{-1}. It is discovered that RG-H exhibits an exception for the kinetic assessment at lower q values due to the aggregation of its structure, which prevents pepsin from penetrating the gel, whereas TG-H digested with 2000 U mL^{-1} pepsin and TG-D digested with 8000 U mL^{-1} exhibit an exception by showing no change in protein aggregation at the nanoscale level at higher q values due to their more homogeneous structure. The change in the structure of the casein gels on the micro- and nanoscales was found to be governed primarily by the access of the pepsin enzyme within the interior of the gel particles. For three samples other than RG-H, increasing pepsin concentration increased the digestion rate. However, it was discovered that increasing the pepsin enzyme concentration does not inherently accelerate the rate of structural transformation, as was observed for RG-H. The *in situ* setup revealed the significance of pepsin accessibility for the digestion of each gel in a distinct manner. Due to its relative sensitivity to acidic environments, rennet gels in H_2O (RG-H) exhibited the most substantial structural change in this instance and only RG-H demonstrated a decrease in the rate of gel network disruption with increasing pepsin concentration (Table 1). Consequently, it is essential to discuss the effect of increasing enzyme concentration in relation to RG-H, where, of all the samples studied, the rate of digestion was fastest for RG-H digested in the presence of 2000 U mL^{-1}. However, unlike other samples, increasing the pepsin concentration from 2000 U mL^{-1} to 8000 U mL^{-1} unexpectedly reduced the rate of digestion. For RG-H, SANS revealed a rapid initial fall in clustering strength, or degree of protein aggregation, and an increase in the correlation length, believed to correspond to the local density of protein stranded clusters at the interior of the casein micelle. The RG-H networks were known to contract into a more densely packed structure with fewer openings leading to reduced surface area for pepsin to

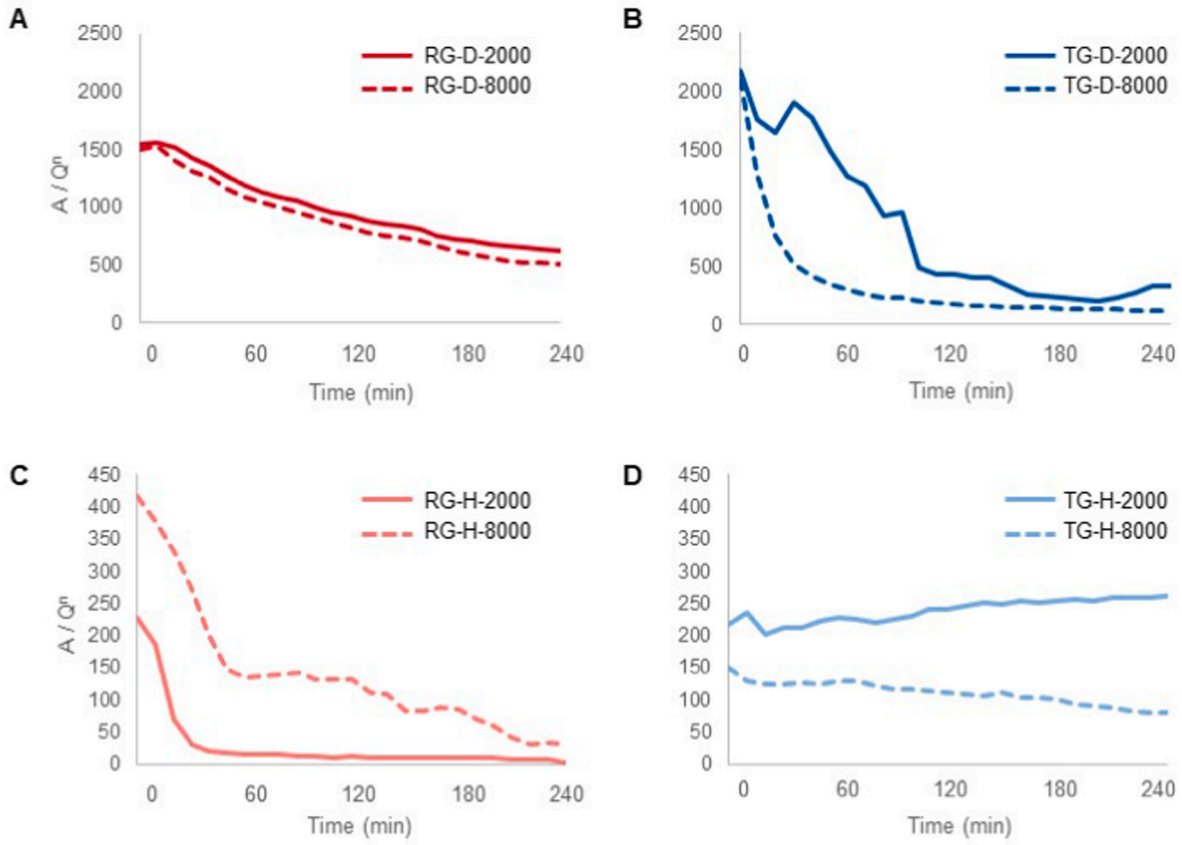

Fig. 6. The clustering strength (A/q^n) at q = 0.002 $Å^{-1}$ of (A) RG-D, (C) RG-H, (B) TG-D and (D) TG-H, during 240 min of simulated gastric digestion with pepsin activity of 2000 (line) and 8000 (dashed line) U mL^{-1}.

penetrate during the initial stage of digestion and digestion progression at the surface only (Bayrak et al., 2021; Floury et al., 2018). Here, the relative sensitivity to an acidic environment might have hindered the diffusion of pepsin within the pores and therefore the excess pepsin at 8000 U mL^{-1} remaining in the liquid phase may have resulted in a loss of activity. The accessible surface area of the gel network decreased, and more pepsin remained in the liquid phase (Mennah-Govela & Bornhorst, 2021) leading to a greater local concentration of pepsin outside the gel, thereby increasing the likelihood of pepsin autolysis. As a result, the compact structure of RG reduced the surface area for pepsin to penetrate and was affected more by the concentration change of pepsin. The rate of digestion (scattering intensity) and degree of protein aggregation (clustering strength) did not decrease as quickly for the rennet-induced gels in D_2O (RG-D) compared to H_2O (RG-H), where gels prepared in D_2O are known to have a more homogenous microstructure than those prepared in H_2O. Bayrak et al. (2021) demonstrated that gels made with D_2O exhibit smaller and more uniform pores through the network structure believed to prevent access of the pepsin enzyme in the liquid phase from penetrating the gel. While the concentration of pepsin did not seem to affect the clustering strength of RG-D (Fig. 6A), the correlation length increased more in 2000 U mL^{-1} compared to 8000 U mL^{-1}. Yet, loosening of the protein gel network for RG seemed to reach the same level after 240 min of digestion at each pepsin concentration, despite the slower decrease in clustering strength in RG-H compared to RG-D. As such, an increase in enzyme concentration does not necessarily result in an increase in digestion rate; and consequently, the aggregation of solid particles that hinder enzyme diffusion must be regarded as a parameter when analysing the kinetics of digestion.

In addition, the *in situ* system demonstrated the importance of physical disruption, which was observed to be more significant for the more brittle gels. For TG-H, increasing pepsin concentration from 2000 U mL^{-1} to 8000 U mL^{-1} showed an increase in digestion rate (higher rate constant *R*), loosening of aggregated micelles (lower A/q^n) and increased density of small protein fragments within the hard regions of casein micelle (higher ξ). Hence, the physical disruption of TG-H was chosen for investigation with USANS, yielding comparable results on a larger scale. In previous rheological studies, TG particles are predominantly affected by physical disruption due to their brittle structure resulting in greater fracturability (Bayrak et al., 2021). Thus, mechanically disruptive effects directly related to the flow of an *in situ* system would be expected to present themselves more in TG than RG, creating a greater surface area for pepsin to act on. A similar effect on brittleness was observed previously with solvent change, where gel stiffness and brittleness are greater in D_2O samples than in H_2O (Bayrak et al., 2021; Larsson, 1988; Oakenfull & Scott, 2003). As such, brittleness has the greatest impact on fracturability for TG compared to RG, where the compactness of the gel structure is unaffected by the acidic environment of the stomach (Bayrak et al., 2021). As a result, TG-D with enhanced brittleness, providing greater surface area and penetration of pepsin in the latter stages, had a greater rate of intensity decrease compared to TG-H. The estimated smaller TG-D particles resulting from the brittle structure may have allowed pepsin diffusion more readily within the gels and led to the greatest increase in the density of protein-stranded clusters, as shown by the greatest increase in correlation length.

While local aggregation of RG in an acidic environment prevents enzyme access, the physical disruption of brittle TG particles in a flowing *in situ* system creates a greater surface area for pepsin. Similarly, the effect of the solvent on the gel structure resulted in variations in digestion rate due to differences in the packing of small protein fragments or the aggregation of nearby clusters. In the presence of an excess pepsin enzyme, a decrease in the surface area slowed the rate of digestion, so it is likely that the increased enzyme concentration caused

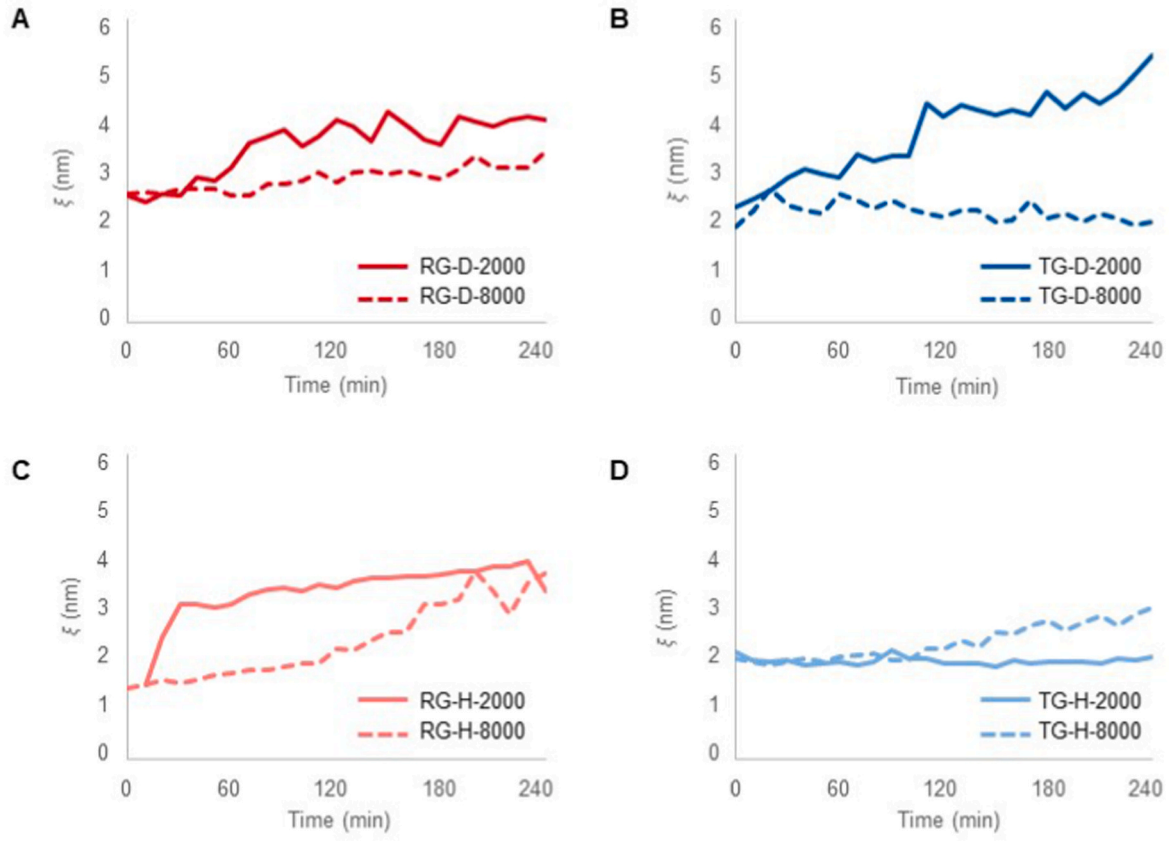

Fig. 7. Correlation length (Å) of (A) RG-D, (C) RG-H, (B) TG-D and (D) TG-H, indicating protein cluster size, during 240 min of simulated gastric digestion with pepsin activity of 2000 (line) and 8000 (dashed line) U mL^{-1}.

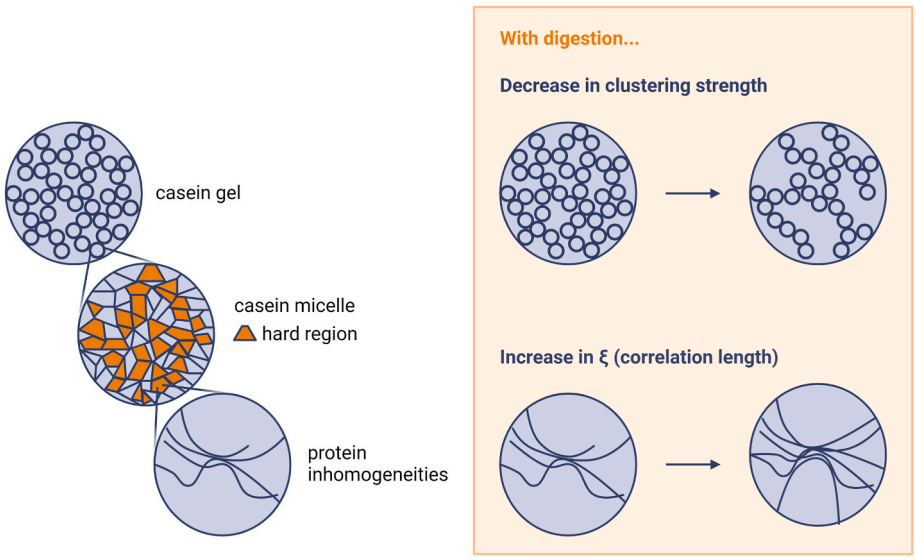

Fig. 8. Schematic representation of the trends in clustering strength and correlation length with digestion for a casein protein gel.

autolysis of pepsin rather than hydrolysis of the casein gel. The reduced effect of higher pepsin concentration (8000 U mL^{-1}) on the structure of gels suggests enzyme autolysis may have occurred, which is known to accelerate under favourable conditions, such as an acidic pH. For example, Qiao, Gumpertz, and Van Kempen (2002) demonstrated that the rate of pepsin activity loss was significantly affected by pH and concentration, with peptide bond breakage occurring more rapidly at lower pH and higher enzyme concentrations. However, in this study, the pH was held constant at pH 3 so pH is not anticipated to influence the enzyme activity. Another study by Qiao, Gumpertz, and Van Kempen (2005) found that in the presence of a protein substrate, enzymes lost activity faster at higher trypsin and chymotrypsin concentrations. It was therefore assumed that increasing the concentration of pepsin is likely to decrease the enzyme's half-life in the absence of casein gel substrates and hence increased proteolysis in all samples. In another study, the pepsin activity of different whey protein gel geometries varied and after

30 and 60 min, the pepsin activity of the larger gel particles was higher due to low buffering capacity causing pH to decrease faster (Mennah--Govela et al., 2021). This was a result of the decreased accessible surface area for pepsin to act on and limited diffusion within the gel particles, leaving more pepsin in the liquid phase. Therefore, we can presume that the inaccessibility of the pepsin enzyme contributed to the preservation of a higher level of activity and autolysis. While this *in situ* setup for neutron scattering could provide extensive information on the kinetics of semi-solid systems, enzyme concentration must be optimised to prevent autolysis.

5. Conclusion

This study is the first attempt to establish a methodology for the *in situ*, real-time measurement of protein gel degradation under simulated gastric digestion conditions using USANS and SANS. Both USANS and low q SANS were employed to provide a kinetic assessment of digestion as a function of time while SANS was employed to provide structural analysis at a smaller length scale. Changing enzyme concentration to observe the kinetic effects of digestion has demonstrated that an increase in pepsin concentration does not necessarily accelerate proteolysis. The inaccessibility of the gel network to gastric fluid, including pepsin, resulted in lower digestion rates as excess pepsin enzyme concentrated in the gastric fluid and likely autolysed. For instance, TG-D gel breaks rapidly due to its brittle nature while RG-H is susceptible to aggregation in an acidic environment. The excess enzyme that is inaccessible within the gel network decreased the hydrolysis rate and increased the likelihood of enzyme autolysis. Increasing the pepsin enzyme concentration to analyse the kinetics of a system would only be effective if the structure is sufficiently fragile to generate a new surface area for the excess enzyme. The enzyme-substrate concentration should be optimised to expect a direct correlation between enzyme concentration and digestibility before using this *in situ* system for kinetic analysis.

The extent of physical disruption observed for each gel under gastric digestion conditions is less using the traditional static *in vitro* methodology due to the comparatively milder force of mixing (Brodkorb et al., 2019) compared to the current study. Furthermore, the variation in the digestion parameters such as duration, pH, number of digestion steps, agitation, and amount of food will influence the outcomes of static digestion models. The circulating system could be easily modified to a semi-dynamic study with the addition of a pH regulation system that permits the regulation of pH rather than maintaining a constant pH of 3 during digestion. Although the flowing system does not fully represent the contraction in the stomach, the current results indicate the process can in part replicate traditional static approaches. However, optimisation for the flow rate is needed to better replicate the mixing of a static system. Also, different modes of coagulation would generate different amino acid compositions during gastric digestion, which would be of interest to study in real-time. Consequently, future modifications to the apparatus to extract small samples in real-time would increase our understanding of the system. This study emphasizes once again the importance of studying the kinetics of digestion at various length scales using a variety of physical disruption techniques. Using this *in situ* setup, several kinetic investigations can be explored in real-time.

Credit author statement

Meltem Bayrak, Conceptualization; Methodology; Investigation; Formal analysis; Writing - original draft; Visualization.

Andrew E. Whitten, Investigation; Methodology; Writing - Review & Editing.

Jitendra Mata, Conceptualization; Supervision; Methodology; Validation; Writing - review & editing.

Charlotte E.Conn, Conceptualization; Supervision; Methodology; Validation; Writing - review & editing.

Juliane Floury, Conceptualization; Supervision; Methodology; Validation; Writing - review & editing.

Amy Logan, Conceptualization; Supervision; Methodology; Validation; Writing - review & editing.

Declaration of competing interest

None.

Data availability

Data will be made available on request.

Acknowledgements

We acknowledge the support of the Australian Nuclear Science and Technology Organisation (ANSTO) in providing USANS and SANS beam facilities (proposal no. DB9587) used in this work. The authors would like to thank AINSE Limited for providing financial assistance (Award – PGRA) to enable work on Quokka and Kookaburra, and the CSIRO AIM Future Science Platform for supporting this work. The authors also acknowledge Norman Booth (ANSTO) for input and assistance with the *in situ* digestion setup for neutron scattering; and Dr. Liliana de Campo, Dr. Michael Page and Dr. Elizabeth Ho (ANSTO Minerals) for their help with equipment.

Appendix A. Supplementary data

Supplementary data to this article can be found online at https://doi.org/10.1016/j.foodhyd.2023.108919.

References

Arnold, O., Bilheux, J.-C., Borreguero, J., Buts, A., Campbell, S. I., Chapon, L., et al. (2014). Mantid—data analysis and visualization package for neutron scattering and μ SR experiments. *Nuclear Instruments and Methods in Physics Research Section A: Accelerators, Spectrometers, Detectors and Associated Equipment, 764*, 156–166.

Barbé, F., Ménard, O., Le Gouar, Y., Buffière, C., Famelart, M.-H., Laroche, B., et al. (2014). Acid and rennet gels exhibit strong differences in the kinetics of milk protein digestion and amino acid bioavailability. *Food Chemistry, 143*, 1–8.

Bayrak, M., Mata, J., Raynes, J. K., Greaves, M., White, J., Conn, C. E., et al. (2021). Investigating casein gel structure during gastric digestion using ultra-small and small-angle neutron scattering. *Journal of Colloid and Interface Science, 594*, 561–574.

Bayrak, M., Mata, J. P., Whitten, A. E., Conn, C. E., Floury, J., & Logan, A. (2022). Physical disruption of gel particles on the macroscale does not affect the study of protein gel structure on the micro or nanoscale. *Colloid and Interface Science Communications, 46*, Article 100574.

Blazek, J., & Gilbert, E. P. (2010). Effect of enzymatic hydrolysis on native starch granule structure. *Biomacromolecules, 11*(12), 3275–3289.

Boland, M., Golding, M., & Singh, H. (2014). *Food structures, digestion and health*. Academic Press.

Bornhorst, G. M., Ferrua, M. J., & Singh, R. P. (2015). A proposed food breakdown classification system to predict food behavior during gastric digestion. *Journal of Food Science, 80*(5), R924–R934.

Bornhorst, G. M., Gouseti, O., Wickham, M. S., & Bakalis, S. (2016). Engineering digestion: Multiscale processes of food digestion. *Journal of Food Science, 81*(3), R534–R543.

Bouchoux, A., Gesan-Guiziou, G., Pérez, J., & Cabane, B. (2010). How to squeeze a sponge: Casein micelles under osmotic stress, a SAXS study. *Biophysical Journal, 99*(11), 3754–3762.

Brodkorb, A., Egger, L., Alminger, M., Alvito, P., Assunção, R., Ballance, S., et al. (2019). INFOGEST static in vitro simulation of gastrointestinal food digestion. *Nature Protocols, 14*(4), 991–1014.

Calbet, J. A., & Holst, J. J. (2004). Gastric emptying, gastric secretion and enterogastrone response after administration of milk proteins or their peptide hydrolysates in humans. *European Journal of Nutrition, 43*(3), 127–139.

Callaghan-Patrachar, N., Peyronel, F., Pink, D., Marangoni, A., & Adams, C. (2021). USANS and SANS investigations on the coagulation of commercial bovine milk: Microstructures induced by calf and fungal rennet. *Food Hydrocolloids, 116*, Article 106622.

Claessens, M., Calame, W., Siemensma, A. D., van Baak, M. A., & Saris, W. H. (2009). The effect of different protein hydrolysate/carbohydrate mixtures on postprandial glucagon and insulin responses in healthy subjects. *European Journal of Clinical Nutrition, 63*(1), 48–56.

Clulow, A. J., Salim, M., Hawley, A., & Boyd, B. J. (2018). A closer look at the behaviour of milk lipids during digestion. *Chemistry and Physics of Lipids, 211*, 107–116.

Dangin, M., Boirie, Y., Guillet, C., & Beaufrère, B. (2002). Influence of the protein digestion rate on protein turnover in young and elderly subjects. *Journal of Nutrition, 132*(10), 3228S–3233S.
Dangin, M., Guillet, C., Garcia-Rodenas, C., Gachon, P., Bouteloup-Demange, C., Reiffers-Magnani, K., et al. (2003). The rate of protein digestion affects protein gain differently during aging in humans. *Journal of Physiology, 549*(2), 635–644.
De Kruif, C. (2014). The structure of casein micelles: A review of small-angle scattering data. *Journal of Applied Crystallography, 47*(5), 1479–1489.
Egger, L., Ménard, O., Baumann, C., Duerr, D., Schlegel, P., Stoll, P., et al. (2019). Digestion of milk proteins: Comparing static and dynamic in vitro digestion systems with in vivo data. *Food Research International, 118*, 32–39.
Farooq, A. M., Li, C., Chen, S., Fu, X., Zhang, B., & Huang, Q. (2018). Particle size affects structural and in vitro digestion properties of cooked rice flours. *International Journal of Biological Macromolecules, 118*, 160–167.
Fatouros, D. G., Deen, G. R., Arleth, L., Bergenstahl, B., Nielsen, F. S., Pedersen, J. S., et al. (2007). Structural development of self nano emulsifying drug delivery systems (SNEDDS) during in vitro lipid digestion monitored by small-angle X-ray scattering. *Pharmaceutical Research, 24*(10), 1844–1853.
Floury, J., Bianchi, T., Thévenot, J., Dupont, D., Jamme, F., Lutton, E., et al. (2018). Exploring the breakdown of dairy protein gels during in vitro gastric digestion using time-lapse synchrotron deep-UV fluorescence microscopy. *Food Chemistry, 239*, 898–910.
Frieberg, B. R., Garatsa, R.-S., Jones, R. L., Bachert, J. O., Crawshaw, B., Liu, X. M., et al. (2018). Viscoplastic fracture transition of a biopolymer gel. *Soft Matter, 14*(23), 4696–4701.
Gebhardt, R., Takeda, N., Kulozik, U., & Doster, W. (2011). Structure and stabilizing interactions of casein micelles probed by high-pressure light scattering and FTIR. *The Journal of Physical Chemistry B, 115*(10), 2349–2359.
Grassby, T., Mandalari, G., Grundy, M. M.-L., Edwards, C. H., Bisignano, C., Trombetta, D., et al. (2017). In vitro and in vivo modeling of lipid bioaccessibility and digestion from almond muffins: The importance of the cell-wall barrier mechanism. *Journal of Functional Foods, 37*, 263–271.
Grundy, M. M., Grassby, T., Mandalari, G., Waldron, K. W., Butterworth, P. J., Berry, S. E., et al. (2015). Effect of mastication on lipid bioaccessibility of almonds in a randomized human study and its implications for digestion kinetics, metabolizable energy, and postprandial lipemia. *The American Journal of Clinical Nutrition, 101*(1), 25–33.
Hammouda, B., Ho, D. L., & Kline, S. (2004). Insight into clustering in poly (ethylene oxide) solutions. *Macromolecules, 37*(18), 6932–6937.
Hammouda, B., Horkay, F., & Becker, M. L. (2005). Clustering and solvation in poly (acrylic acid) polyelectrolyte solutions. *Macromolecules, 38*(5), 2019–2021.
Holt, C., De Kruif, C., Tuinier, R., & Timmins, P. (2003). Substructure of bovine casein micelles by small-angle X-ray and neutron scattering. *Colloids and Surfaces A: Physicochemical and Engineering Aspects, 213*(2–3), 275–284.
Hong, L., & Salentinig, S. (2022). Functional food colloids: Studying structure and interactions during digestion. *Current Opinion in Food Science, 45*, Article 100817.
Huang, X., Terech, P., Raghavan, S. R., & Weiss, R. G. (2005). Kinetics of 5α-cholestan-3β-yl N-(2-naphthyl) carbamate/n-alkane organogel formation and its influence on the fibrillar networks. *Journal of the American Chemical Society, 127*(12), 4336–4344.
Hussain, I., Bell, A. E., & Grandison, A. S. (2013). Mozzarella-type curd made from Buffalo, cows' and ultrafiltered cows' milk. 1. rheology and Microstructure. *Food and Bioprocess Technology, 6*(7), 1729–1740.
Ingham, B., Smialowska, A., Erlangga, G. D., Matia-Merino, L., Kirby, N., Wang, C., et al. (2016). Revisiting the interpretation of casein micelle SAXS data. *Soft Matter, 12*(33), 6937–6953.
Jalabert-Malbos, M.-L., Mishellany-Dutour, A., Woda, A., & Peyron, M.-A. (2007). Particle size distribution in the food bolus after mastication of natural foods. *Food Quality and Preference, 18*(5), 803–812.
Kent, M., Cheng, G., Murton, J., Carles, E., Dibble, D., Zendejas, F., et al. (2010). Study of enzymatic digestion of cellulose by small angle neutron scattering. *Biomacromolecules, 11*(2), 357–368.
Khan, J., Hawley, A., Rades, T., & Boyd, B. J. (2016). In situ lipolysis and synchrotron small-angle X-ray scattering for the direct determination of the precipitation and solid-state form of a poorly water-soluble drug during digestion of a lipid-based formulation. *Journal of Pharmaceutical Sciences, 105*(9), 2631–2639.
Kong, F., & Singh, R. P. (2009). Modes of disintegration of solid foods in simulated gastric environment. *Food Biophysics, 4*(3), 180–190.
Larsson, U. (1988). Polymerization and gelation of fibronogen in D2O. *European Journal of Biochemistry, 174*(1), 139–144.
Lazzaro, F., Bouchoux, A., Raynes, J., Williams, R., Ong, L., Hanssen, E., et al. (2020). Tailoring the structure of casein micelles through a multifactorial approach to manipulate rennet coagulation properties. *Food Hydrocolloids, 101*, Article 105414.
Li, Y., Li, M., Wang, L., & Li, Z. (2022). Effect of particle size on the release behavior and functional properties of wheat bran phenolic compounds during in vitro gastrointestinal digestion. *Food Chemistry, 367*, Article 130751.
Liu, D., Dhital, S., Wu, P., Chen, X.-D., & Gidley, M. J. (2019). In vitro digestion of apple tissue using a dynamic stomach model: Grinding and crushing effects on polyphenol bioaccessibility. *Journal of Agricultural and Food Chemistry, 68*(2), 574–583.
Li, Q., & Zhao, Z. (2019). Acid and rennet-induced coagulation behavior of casein micelles with modified structure. *Food Chemistry, 291*, 231–238.
Lyu, Y., Bi, J., Chen, Q., Wu, X., Qiao, Y., Hou, H., et al. (2021). Bioaccessibility of carotenoids and antioxidant capacity of seed-used pumpkin byproducts powders as affected by particle size and corn oil during in vitro digestion process. *Food Chemistry, 343*, Article 128541.
Mackie, A. R., Rafiee, H., Malcolm, P., Salt, L., & van Aken, G. (2013). Specific food structures supress appetite through reduced gastric emptying rate. *American Journal of Physiology - Gastrointestinal and Liver Physiology, 304*(11), G1038–G1043.
Mandalari, G., Merali, Z., Ryden, P., Chessa, S., Bisignano, C., Barreca, D., et al. (2018). Durum wheat particle size affects starch and protein digestion in vitro. *European Journal of Nutrition, 57*(1), 319–325.
Marchin, S., Putaux, J.-L., Pignon, F., & Léonil, J. (2007). Effects of the environmental factors on the casein micelle structure studied by cryo transmission electron microscopy and small-angle x-ray scattering/ultrasmall-angle x-ray scattering. *The Journal of Chemical Physics, 126*(4), Article 01B617.
Mata, J. P., Udabage, P., & Gilbert, E. P. (2011). Structure of casein micelles in milk protein concentrate powders via small angle X-ray scattering. *Soft Matter, 7*(8), 3837–3843.
Mellema, M., Heesakkers, J., Van Opheusden, J., & Van Vliet, T. (2000). Structure and scaling behavior of aging rennet-induced casein gels examined by confocal microscopy and permeametry. *Langmuir, 16*(17), 6847–6854.
Mennah-Govela, Y. A., & Bornhorst, G. M. (2021). Breakdown mechanisms of whey protein gels during dynamic in vitro gastric digestion. *Food & Function, 12*(5), 2112–2125.
Morifuji, M., Ishizaka, M., Baba, S., Fukuda, K., Matsumoto, H., Koga, J., et al. (2010). Comparison of different sources and degrees of hydrolysis of dietary protein: Effect on plasma amino acids, dipeptides, and insulin responses in human subjects. *Journal of Agricultural and Food Chemistry, 58*(15), 8788–8797.
Mulet-Cabero, A.-I., Egger, L., Portmann, R., Ménard, O., Marze, S., Minekus, M., et al. (2020). A standardised semi-dynamic in vitro digestion method suitable for food–an international consensus. *Food & Function, 11*(2), 1702–1720.
Nishijima, H., Tomota, Y., Su, Y., Gong, W., & Suzuki, J.-i. (2016). Monitoring of bainite transformation using in situ neutron scattering. *Metals, 6*(1), 16.
Norton, J. E., Wallis, G. A., Spyropoulos, F., Lillford, P. J., & Norton, I. T. (2014). Designing food structures for nutrition and health benefits. *Annual Review of Food Science and Technology, 5*, 177–195.
Oakenfull, D., & Scott, A. (2003). Gelatin gels in deuterium oxide. *Food Hydrocolloids, 17*(2), 207–210.
Qiao, Y., Gumpertz, M., & Van Kempen, T. (2002). Stability of pepsin (EC 3.4. 23.1) during in vitro protein digestibility assay 1, 2. *Journal of Food Biochemistry, 26*(4), 355–375.
Qiao, Y., Gumpertz, M., & Van Kempen, T. (2005). Stability of a pancreatic enzyme cocktail during in vitro protein digestibility assays. *Journal of Food Biochemistry, 29*(2), 205–220.
Randle, R. I., Fuentes-Caparrós, A. M., Cavalcanti, L. P., Schweins, R., Adams, D. J., & Draper, E. R. (2022). Investigating aggregation using in situ electrochemistry and small-angle neutron scattering. *Journal of Physical Chemistry C, 126*(31), 13427–13432.
Rasid, I. M., Do, C., Holten-Andersen, N., & Olsen, B. D. (2021). Effect of sticker clustering on the dynamics of associative networks. *Soft Matter, 17*(39), 8960–8972.
Rehm, C., Campo, L.d., Brûlé, A., Darmann, F., Bartsch, F., & Berry, A. (2018). Design and performance of the variable-wavelength Bonse–Hart ultra-small-angle neutron scattering diffractometer KOOKABURRA at ANSTO. *Journal of Applied Crystallography, 51*(1), 1–8.
Rezhdo, O., Di Maio, S., Le, P., Littrell, K. C., Carrier, R. L., & Chen, S.-H. (2017). Characterization of colloidal structures during intestinal lipolysis using small-angle neutron scattering. *Journal of Colloid and Interface Science, 499*, 189–201.
Roefs, S., de Groot-Mostert, A., & Van Vliet, T. (1990). Structure of acid casein gels 1. Formation and model of gel network. *Colloids and Surfaces, 50*, 141–159.
Saffer, E. M., Lackey, M. A., Griffin, D. M., Kishore, S., Tew, G. N., & Bhatia, S. R. (2014). SANS study of highly resilient poly (ethylene glycol) hydrogels. *Soft Matter, 10*(12), 1905–1916.
Salentinig, S., Amenitsch, H., & Yaghmur, A. (2017). In situ monitoring of nanostructure formation during the digestion of mayonnaise. *ACS Omega, 2*(4), 1441–1446.
Salentinig, S., Phan, S., Hawley, A., & Boyd, B. J. (2015). Self-assembly structure formation during the digestion of human breast milk. *Angewandte Chemie, 127*(5), 1620–1623.
Salentinig, S., Phan, S., Khan, J., Hawley, A., & Boyd, B. J. (2013). Formation of highly organized nanostructures during the digestion of milk. *ACS Nano, 7*(12), 10904–10911.
Schorsch, C., Jones, M., & Norton, I. (2002). Micellar casein gelation at high sucrose content. *Journal of Dairy Science, 85*(12), 3155–3163.
Singh, R., Hemar, Y., Gilbert, E. P., Wu, Z., & Yang, Z. (2020). Effect of genipin cross-linking on the structural features of skim milk in the presence of ethylenediaminetetraacetic acid (EDTA). *Colloids and Surfaces A: Physicochemical and Engineering Aspects, 603*, Article 125174.
Singh, H., Ye, A., & Ferrua, M. J. (2015). Aspects of food structures in the digestive tract. *Current Opinion in Food Science, 3*, 85–93.
Sokolova, A., Whitten, A. E., de Campo, L., Christoforidis, J., Eltobaji, A., Barnes, J., et al. (2019). Performance and characteristics of the BILBY time-of-flight small-angle neutron scattering instrument. *Journal of Applied Crystallography, 52*(1), 1–12.
Somaratne, G., Ferrua, M. J., Ye, A., Nau, F., Floury, J., Dupont, D., et al. (2020). Food material properties as determining factors in nutrient release during human gastric digestion: A review. *Critical Reviews in Food Science and Nutrition, 60*(22), 3753–3769.
Sørensen, H., Pedersen, J. S., Mortensen, K., & Ipsen, R. (2013). Characterisation of fractionated skim milk with small-angle X-ray scattering. *International Dairy Journal, 33*(1), 1–9.
Stefaniuk, A., Gawinkowski, S., Golec, B., Gorski, A., Szutkowski, K., Waluk, J., et al. (2022). Isotope effects observed in diluted D2O/H2O mixtures identify HOD-induced low-density structures in D2O but not H2O. *Scientific Reports, 12*(1), Article 18732.

Warren, D. B., Anby, M. U., Hawley, A., & Boyd, B. J. (2011). Real time evolution of liquid crystalline nanostructure during the digestion of formulation lipids using synchrotron small-angle X-ray scattering. *Langmuir, 27*(15), 9528–9534.

Xu, J., Li, Z., Zhong, Y., Zhou, Q., Lv, Q., Chen, L., et al. (2021). The effects of molecular fine structure on rice starch granule gelatinization dynamics as investigated by in situ small-angle X-ray scattering. *Food Hydrocolloids, 121*, Article 107014.

Yaghmur, A., Lotfi, S., Ariabod, S. A., Bor, G., Gontsarik, M., & Salentinig, S. (2019). Internal lamellar and inverse hexagonal liquid crystalline phases during the digestion of krill and astaxanthin oil-in-water emulsions. *Frontiers in Bioengineering and Biotechnology, 7*, 384.

Yang, Z., de Campo, L., Gilbert, E. P., Knott, R., Cheng, L., Storer, B., et al. (2021). *Effect of NaCl and CaCl2 concentration on the rheological and structural characteristics of thermally-induced quinoa protein gels*. Food Hydrocolloids, Article 107350.

Yang, Z., de Campo, L., Gilbert, E. P., Knott, R., Cheng, L., Storer, B., et al. (2022). Effect of NaCl and CaCl2 concentration on the rheological and structural characteristics of thermally-induced quinoa protein gels. *Food Hydrocolloids, 124*, Article 107350.

Yang, Z., Hemar, Y., Hilliou, L., Gilbert, E. P., McGillivray, D. J., Williams, M. A., et al. (2016). Nonlinear behavior of gelatin networks reveals a hierarchical structure. *Biomacromolecules, 17*(2), 590–600.

Yang, S., Tyler, A. I., Ahrné, L., & Kirkensgaard, J. J. (2021). Skimmed milk structural dynamics during high hydrostatic pressure processing from in situ SAXS. *Food Research International, 147*, Article 110527.

Ye, A., Cui, J., Dalgleish, D., & Singh, H. (2016). Formation of a structured clot during the gastric digestion of milk: Impact on the rate of protein hydrolysis. *Food Hydrocolloids, 52*, 478–486.

Zhang, Y., Li, Y., Wang, P., Tian, Y., Liang, Q., & Ren, F. (2017). Rennet-induced coagulation properties of yak casein micelles: A comparison with cow casein micelles. *Food Research International, 102*, 25–31.